A simplified approach to include confinement induced band structure changes into the NsFET compact model

Aishwarya Singh
Electrical Engineering
IIT Gandhinagar
Gandhinagar, India
singh_aishwarya@iitgn.ac.in

Mohit D. Ganeriwala
Electronics and Computer Technology
Universidad de Granada
Granada, Spain
mohit@ugr.es

Ramandeep Kaur
Electrical Engineering
IIT Gandhinagar
Gandhinagar, India
ramandeep.kaur@iitgn.ac.in

Nihar R. Mohapatra
Electrical Engineering
IIT Gandhinagar
Gandhinagar, India
nihar@iitgn.ac.in

PREPRINT

***Abstract*—This work presents a simplified mathematical method to capture the k.p-based band structure modifications with confinement and device substrate/transport orientation in the compact model of quantum confined Nanosheet FETs. The change in effective mass with confinement is captured in terms of non-parabolic sub-bands. The estimated sub-bands are used to compute inversion charge density and gate capacitance using a bottom–up scalable compact model for different device dimensions and substrate/channel orientations. The accuracy of the proposed method is confirmed using k.p simulation in Global TCAD Solutions (GTS).**

***Index Terms*—non-parabolic subbands, nanosheet FET, k.p based bandstructure, quantum confinement, channel orientation, effective mass, bottom-up scalable compact model**

I. Introduction

The Silicon Nanosheet FETs (NsFET) have been identified by the semiconductor industry as the leading architecture to continue CMOS technology scaling beyond the 5 nm node [1]. The NsFETs offer excellent gate electrostatics with negligible short-channel effects. Fig. 1 shows schematic diagram of a NsFET with the extremely thin body (H) and width (W). For such a confined system, the Quantum Mechanical Confinement (QMC) induced effects play a major role in device performance. The QMC causes the separation of energy bands, resulting in sub-band formation and thereby affecting the density of states (DOS). Unlike the bulk MOSFETs, energy bands in confined structure can no longer be considered as a continuous 3D stack of energies. This affects the inversion charge density and this phenomena is more pronounced in thin and narrow NsFETs.

Fig. 2 shows the E-K diagram of a (100)/[110] oriented silicon channel. Here, two out of the six valleys (as shown in Fig. 3), residing in the confinement direction (x-y in Fig. 1), are projected at the Γ point (k_z = 0). The pair of two-fold degenerate valleys are projected at the off-Γ axis. Note that only the lowest energy sub-band in each valley is shown. As shown, the relative position of the bands as well as their curvature changes with confinement. This results in the change of the sub-band energies, effective mass and DOS. In addition, these variations are different for each substrate/channel orientation [2]. Moreover, due to the non planar nature of the NsFET channel, the channel's vertical and horizontal side wall has different crystallographic orientations. Therefore, these different orientations need to be properly considered. Note that all the orientations mentioned in this work are along the length of the channel.

Mohit D. Ganeriwala would like to acknowledge the funding from the European Union's Horizon 2020 research and innovation program under the Marie Sklodowska-Curie grant agreement number 101032701

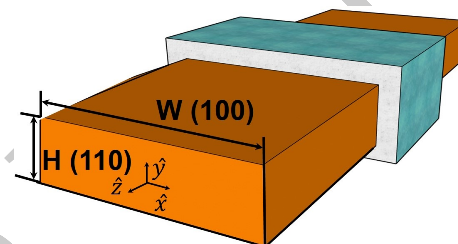

Fig. 1: Cross sectional view of a NsFET confined in the x-y direction. W and H are width and thickness of NsFET respectively. The vertical and horizontal sidewall of the channel has different crystallographic orientation.

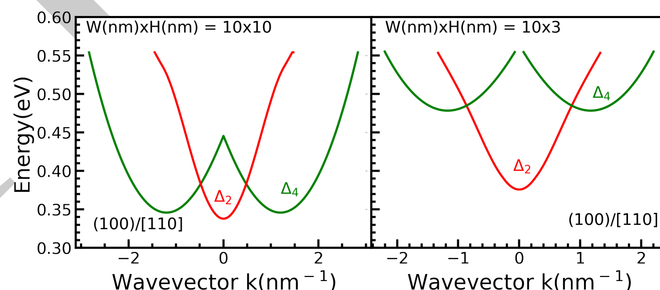

Fig. 2: The k.p based E-K diagram for Si channel oriented in (100)/[110] direction for W (nm) x H (nm) = 10x10 and 10x3. Two fold degenerate band (Δ_2) in confinement direction are projected at Γ (k_z = 0) and pair of two fold degenerate band (Δ_4) at off-Γ (negative and positive k_z respectively).

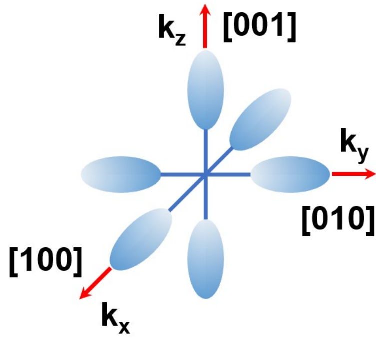

Fig. 3: Six equivalent energy ellipsoids of bulk Silicon oriented in k_x, k_y and k_z directions.

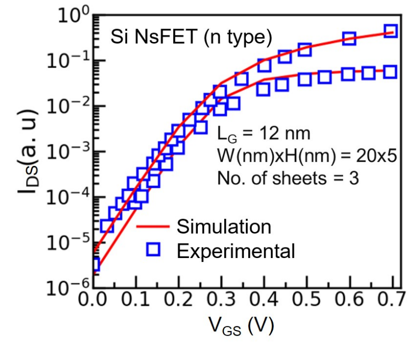

Fig. 4: Drain current (I_{DS}) as a function of V_{GS} for a NsFET with three sheets and W (nm) x H (nm) = 20x5, gate length (L_G) = 12 nm for V_{DS} = 50 mV and 0.7 V. The symbols represent the TCAD data and solid lines represent the experimental data [6]. The TCAD deck is well calibrated against the experimental data.

In earlier literature, it has been shown that the conventional model for bulk MOSFETs needs to be modified to accurately reproduce the NsFET characteristics [3], [4]. The sub-band information has to be accurately calculated and included in the compact model. Since both H and W change with technology or device/circuit design, anywhere from a few to several 100 sub-band energy levels needs to be calculated for the model to seamlessly scale from thin to thick and narrow to wide NsFETs. The BSIM extension for NsFETs uses an empirical equation to calculate sub-band energy levels that require several fitting parameters [3]. In addition, an empirical fitting is used to capture the effective mass change with the confinement. Several reports to model the change in effective mass with confinement are available. However, almost all of them use curve fitting to experimental or simulation data [5]. Further, as such calculations are required for every valley, which differs depending on substrate/channel orientation, this requires extensive fitting as well as different equations to match the characteristics. Such extensive use of fitting parameters not only make the model prone to convergence issues but also makes it complicated and empirical (by losing physical insight).

Recently, a bottom-up compact model has been reported for the NsFETs, which modifies the energy calculation equation of an infinite potential well to capture the wave-function penetration in an explicit manner [4]. This allows for the accurate calculation of any number of sub-bands without the use of fitting parameter, making the model computationally efficient and scalable. However, the proposed model in [4] uses an average DOS effective mass and does not include the effect of orientation and thickness/width scaling.

In this work, we have shown that the problem of change in effective mass with confinement can be formulated in terms of having non-parabolic sub-bands. Therefore, by modifying the widely used non-parabolic effective mass approximation, all the effects discussed above can be included in the compact model. The model [4] is then extended to calculate the sub-band energy explicitly using only a couple of additional fitting parameters. This method makes the model simple, computationally efficient and predictable.

II. Simulation Setup

The simulated NsFET device (shown in Fig. 1) is confined in the x-y direction with transport in the z-direction. The simulations are done using the Global TCAD Solutions (GTS) framework [7]. The TCAD deck is first calibrated with the NsFET experimental data obtained from [6]. Fig. 4 shows the calibrated drain current for a 12 nm long n-type NsFET with three sheets and W (nm) x H (nm) = 20x5 for both linear (V_{DS} = 50 mV) and saturation (V_{DS} = 0.7 V) region. The calibrated deck is then used to simulate the 2D cut surface of single sheet NsFETs with different H, W and surface orientations. The k.p along with the Poisson equation is used to simulate the electrostatic characteristics. This methodology accurately captures the QMC effects such as sub-band energy change, valley splitting, and effective mass variations. The compact model proposed in [4] is used as the baseline model, which is then modified using the approximation proposed to match the k.p simulation data.

III. Methodology

The energy value of the sub-band can be calculated as,

$$E_{i,j} = \frac{\hbar^2}{2m^*}\left[\left(\frac{i\pi}{W_b}\right)^2 + \left(\frac{j\pi}{H_b}\right)^2\right] \quad (1)$$

Here, the subscript i, j indicates i^{th} and j^{th} sub-bands, $\hbar$ is the reduced Planck's constant, m^* is the average DOS effective mass, W_b and H_b are the modified width and height respectively as reported in [4]. Fig. 5 shows the simulated gate capacitance (C_{gg}) for (100)/[110] oriented silicon channel NsFETs with W (nm) x H (nm) = 10x3 and 3x3 using both k.p and the model developed in [4]. The model in [4] uses (1) for sub-band energy calculation. The observed deviation from k.p simulation is due to the assumption of average DOS effective mass in (1). The average DOS effective mass affects both the lowest energy subband level and DOS, thus directly affecting the threshold voltage of the device.

PREPRINT

TABLE I: Confined (x-y direction) and Transport (z direction) effective mass of Silicon ellipsoidal valleys in different substrate/transport orientation

Orientation	Principal axis	Valley	m_x*	m_y*	m_z*
(100)/[110]	Along k_x	E - 1,2	$2m_lm_t/(m_l+m_t)$	m_t	$(m_l+m_t)/2$
	Along k_y	E - 3,4	$2m_lm_t/(m_l+m_t)$	m_t	$(m_l+m_t)/2$
	Along k_z	E - 5,6	m_t	m_l	m_t
(100)/[100]	Along k_x	E - 1,2	m_t	m_t	m_l
	Along k_y	E - 3,4	m_l	m_t	m_t
	Along k_z	E - 5,6	m_t	m_l	m_t
(110)/[100]	Along k_x	E - 1,2	$(m_l+m_t)/2$	$2m_lm_t/(m_l+m_t)$	m_t
	Along k_y	E - 3,4	$(m_l+m_t)/2$	$2m_lm_t/(m_l+m_t)$	m_t
	Along k_z	E - 5,6	m_t	m_t	m_l
(110)/[110]	Along k_x	E - 1,2	m_t	$2m_lm_t/(m_l+m_t)$	$(m_l+m_t)/2$
	Along k_y	E - 3,4	m_t	$2m_lm_t/(m_l+m_t)$	$(m_l+m_t)/2$
	Along k_z	E - 5,6	m_l	m_t	m_t

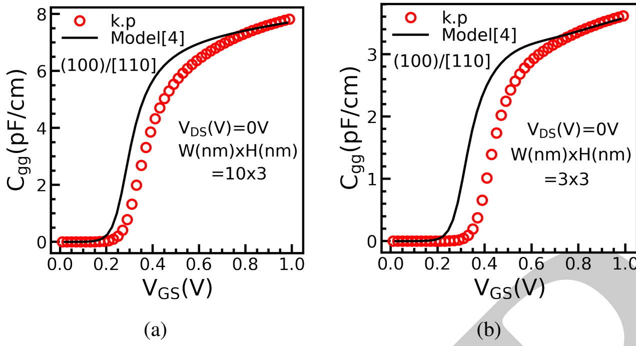

Fig. 5: Gate capacitance (C_{gg}) for (100)/[110] oriented NsFET with W(nm) x H(nm), (a) 10x3 and (b) 3x3 using k.p (open circles) and model [4] (solid lines). The deviation in C_{gg} is due to the assumption of average DOS effective mass in model [4].

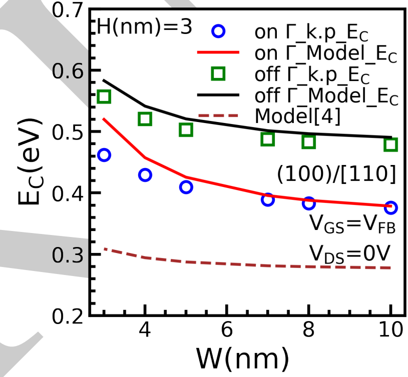

Fig. 6: Variation of conduction band minima E_c with respect to W using k.p (symbols), (2) (solid lines) and (1) (dotted line) for H = 3 nm for both Γ and off-Γ valleys for (100)/[110] orientation.

Therefore, to capture the effect of device orientation on sub-band energy levels, (1) needs to be modified by introducing orientation dependent effective mass. The modified equation can be written as below.

$$E_{i,j} = \frac{i^2\hbar^2}{2m_x^*}\left(\frac{\pi}{W_b}\right)^2 + \frac{j^2\hbar^2}{2m_y^*}\left(\frac{\pi}{H_b}\right)^2 \quad (2)$$

Here, m_x^*, m_y^* are confined effective masses in x and y directions respectively. It can be calculated by using the effective masses associated with the principal axis of ellipsoids (transverse (m_t) and longitudinal (m_l) effective mass). Generally, due to the non-alignment of the principal axis of ellipsoids with substrate/channel orientation, these effective masses are tensor quantities [8]. To relate the effective mass involved in the device coordinate system with the effective mass associated with ellipsoids, a rotation matrix is used in this work. This transforms the ellipsoid coordinate system into the device coordinate system and results in the formation of the inverse effective mass tensor symmetric matrix in the device coordinate system. Using this matrix, effective mass can be computed for any arbitrarily oriented device in both confined directions and transport directions. Table I shows the effective mass of Silicon ellipsoidal valleys shown in Fig. 3 in terms of bulk m_l ($0.89m_0$, m_0 is the rest mass of an electron) and m_t ($0.19m_0$) for different substrate/transport orientations.

Fig. 6 shows the variation of ground state energy (conduction band minima (E_c)) for NsFET with H = 3 nm and varying W. It corresponds to NsFET of dimension W (nm) x H (nm) = 10x3 with quasi 2D channel to NsFETs of dimension 3x3 with quasi 1D channel. Here the symbols and the dotted line shows E_c obtained from the k.p simulations and the original equation (1) as proposed in [4], which uses the average DOS effective mass. It can be seen that the average DOS effective mass not only fails to capture the variation of effective mass with thickness, but it is also erroneous for W = 10 nm. The modification of [4] as given in (2) with the use of m_x^* and m_y^*

PREPRINT

presented in Table I is plotted using solid lines in Fig. 6. The modified model accurately predicts the value of E_c for W = 10 nm for both Γ and off-Γ valleys. However, it still does not capture the accurate variation of effective mass with W.

A. Modified Effective Mass Approach

Due to confinement, the effective mass is not constant with thickness [2]. This behavior can be mimicked using the non-parabolic correction for E-K dispersion. The non-parabolic correction increases the effective mass with energy [9], whereas in the confined system, the effective mass changes with the reduction in thickness. Further, with the confinement, the energy of the sub-band also increases along with the change in the curvature of E-K. Therefore, we are looking at sub-bands with higher effective mass, which are also higher in energy with respect to the unconfined structure. Hence, if the non-parabolic correction equation is modified in such a way that it changes the effective mass with the same energy which corresponds to the desired energy of E-K for reduced thickness, the change in effective mass with the reduction in thickness could also be captured. The energy calculation can thus be modified using the method proposed in [10] as,

$$E_{i,j}^{mod} = E_{i,j}^{NP} + \frac{-1 + \sqrt{1 + 4\alpha_1 \frac{\hbar^2 k_z^2}{2m_z^*}}}{2\alpha_1} \tag{3}$$

Here, k_z and m_z^* are the wave vector and effective mass at the bottom of sub-band in the transport direction (z). $E_{i,j}^{NP}$ denotes the sub-band energy minima at k_z = 0 and can be written as,

$$E_{i,j}^{NP} = U_{i,j} + \frac{-1 + \sqrt{1 + 4\alpha_2 \left(E_{i,j} - U_{i,j}\right)}}{2\alpha_2} \tag{4}$$

Here, $E_{i,j}$ can be calculated using (2), $U_{i,j}$ is the expectation value of potential energy with respect to wave function of ith, j^{th} sub-bands ($\Psi_{i,j}$) and α_1, α_2 are used as fitting parameters. The $U_{i,j}$ for NsFET is calculated as,

$$U_{i,j} = \left\langle \Psi_{i,j}^* | \tilde{\Phi} | \Psi_{i,j} \right\rangle \tag{5}$$

where, $\tilde{\Phi}$ is the perturbing potential as explained in [4]. The final expression after solving (5) is,

$$U_{i,j} = \frac{qQ_{inv}}{4C_c} \tag{6}$$

Here, Q_{inv} is inversion charge density and C_c is centroid capacitance [4]. The Q_{inv} involved in (6) can be calculated using (3) and utilizing the approach explained in [10]. It is given as,

$$Q_{inv} = -q\left[C_{q1}\sum_{i,j} F_{-\frac{1}{2}}\left(\frac{q\Phi_c - Eg_{i,j}^{mod} - Ee_{i,j}^{mod}}{k_B T}\right) + C_{q2}\sum_{i,j} F_{\frac{1}{2}}\left(\frac{q\Phi_c - Eg_{i,j}^{mod} - Ee_{i,j}^{mod}}{k_B T}\right)\right] \tag{7}$$

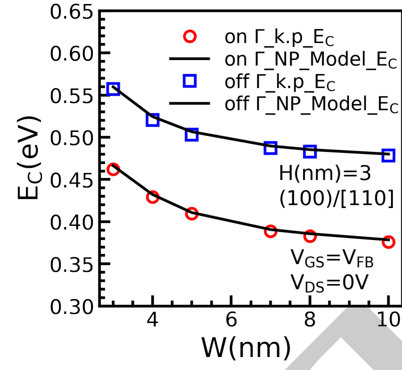

Fig. 7: Variation of conduction band minima (E_c) with respect to W using k.p (symbols) and (3) (solid lines) for H = 3 nm for Γ valley for (100)/[110] orientation. The modified sub-band energy (3) fits the simulation data very well.

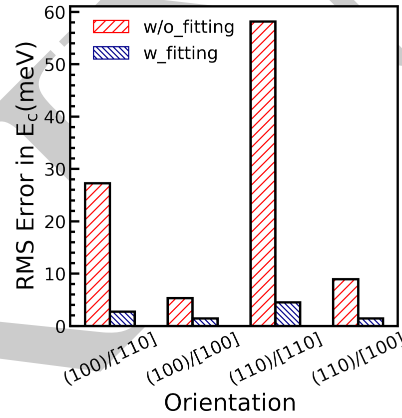

Fig. 8: Root mean square (RMS) error in conduction band minima (E_c) calculation for different device orientation for W (nm) x H (nm) = 10x3 to 3x3 without fitting (2) and with fitting (3). The significant reduction in error can be seen on using the proposed model.

Here, C_{q1} and C_{q2} are the constants [10], Φ_c is the potential at the center of NsFET (x,y = 0), $Eg_{i,j}^{mod}$ is the sub-band energy level considering only geometrical confinement given by (4), $Ee_{i,j}^{mod}$ corresponds to electrical confinement [10], $F_{-1/2}$, $F_{1/2}$ is the Fermi-Dirac integral of order -1/2 and 1/2, k_B is Boltzmann constant and T is temperature.

Fig. 7 shows the variation of E_c with W obtained from the k.p simulation and from (3). It can be seen that the modeled E_c matches with the k.p simulation results and accurately captures the variation of effective mass with confinement. Fig. 8 shows the root mean square (RMS) error for different orientations of NsFET ranging from W (nm) x H (nm) = 10x3 to 3x3. It can be seen that the error is significantly reduced using (3) for all the different combinations of substrate/channel orientation.

IV. Results and Discussion

The modified energy expression (3) and charge expression (7) integrated with compact model in [4] is used for esti-

PREPRINT

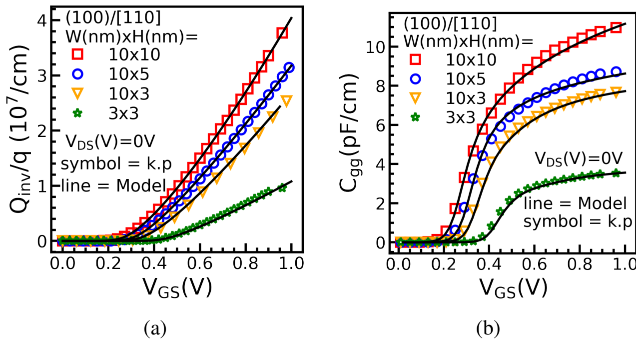

(a) (b)

Fig. 9: (a) Inversion charge density (Q_{inv}) and (b) gate capacitance (C_{gg}) as a function of V_{GS} for NsFET with different dimensions in (100)/[110] orientation. The model is in good agreement with k.p simulation data.

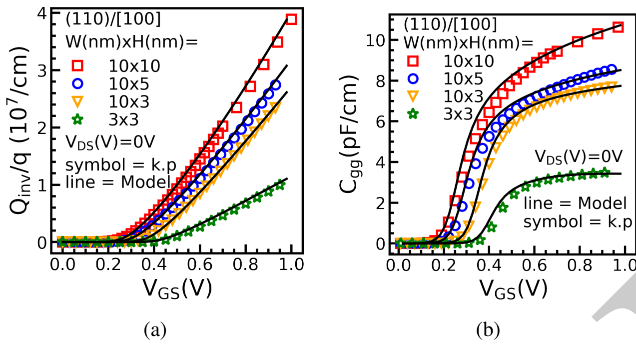

(a) (b)

Fig. 10: (a) Inversion charge density (Q_{inv}) and (b) gate capacitance (C_{gg}) as a function of V_{GS} for NsFET with different dimensions in (110)/[100] orientation. The model is in good agreement with k.p simulation data.

mating the electrostatics behavior of NsFETs. Fig. 9 shows the Q_{inv} and C_{gg} for NsFETs with H = 3 nm and varying W for (100)/[110] device orientation. The model is in good agreement with the k.p simulation data. Therefore, the method proposed here can capture the variation of effective mass using simplified equation with only two fitting parameters. Fig. 10 shows the Q_{inv} and C_{gg} for (110)/[100] device orientation. The good agreement with simulation data confirms that the proposed model is equally accurate for different substrate/channel orientations.

V. Conclusion

To summarize, a modified approach was proposed to compute sub-band energy levels in quantum confined system. It was shown that the proposed approach can be used for different device dimensions and substrate/transport orientations with only two fitting parameters. The proposed model captured the effect of effective mass change with confinement on energies while ensuring the simplicity of compact model. The modified sub-bands were used to compute the NsFET electrostatics using bottom-up scalable compact model [4]. The data from the modified model agreed very well with the data from k.p simulations thereby confirming the accuracy of the model.

References

[1] M. A. Breton, D. Schmidt, A. Greene, J. Frougier, and N. Felix, “Review of nanosheet metrology opportunities for technology readiness,” *Journal of Micro/Nanopatterning, Materials, and Metrology*, vol. 21, no. 2, p. 021206, 2022. [Online]. Available: https://doi.org/10.1117/1.JMM.21.2.021206

[2] N. Neophytou, A. Paul, M. S. Lundstrom, and G. Klimeck, “Bandstructure effects in silicon nanowire electron transport,” *IEEE Transactions on Electron Devices*, vol. 55, no. 6, pp. 1286–1297, 2008. [Online]. Available: https://doi.org/0.1109/TED.2008.920233

[3] A. Dasgupta, S. S. Parihar, P. Kushwaha, H. Agarwal, M.-Y. Kao, S. Salahuddin, Y. S. Chauhan, and C. Hu, “BSIM compact model of quantum confinement in advanced nanosheet FETs,” *IEEE Transactions on Electron Devices*, vol. 67, no. 2, pp. 730–737, 2020. [Online]. Available: https://doi.org/10.1109/TED.2019.2960269

[4] M. D. Ganeriwala, A. Singh, A. Dubey, R. Kaur, and N. R. Mohapatra, “A bottom-up scalable compact model for quantum confined nanosheet FETs,” *IEEE Transactions on Electron Devices*, vol. 69, no. 1, pp. 380–387, 2022. [Online]. Available: https://doi.org/10.1109/TED.2021.3130015

[5] T. Dutta, S. Kumar, P. Rastogi, A. Agarwal, and Y. S. Chauhan, “Impact of channel thickness variation on bandstructure and source-to-drain tunneling in ultra-thin body III-V MOSFETs,” *IEEE Journal of the Electron Devices Society*, vol. 4, no. 2, pp. 66–71, 2016. [Online]. Available: https://doi.org/10.1109/JEDS.2016.2522981

[6] N. Loubet, T. Hook, P. Montanini, C.-W. Yeung, S. Kanakasabapathy, M. Guillom, T. Yamashita, J. Zhang, X. Miao, J. Wang, A. Young, R. Chao, M. Kang, Z. Liu, S. Fan, B. Hamieh, S. Sieg, Y. Mignot, W. Xu, S.-C. Seo, J. Yoo, S. Mochizuki, M. Sankarapandian, O. Kwon, A. Carr, A. Greene, Y. Park, J. Frougier, R. Galatage, R. Bao, J. Shearer, R. Conti, H. Song, D. Lee, D. Kong, Y. Xu, A. Arceo, Z. Bi, P. Xu, R. Muthinti, J. Li, R. Wong, D. Brown, P. Oldiges, R. Robison, J. Arnold, N. Felix, S. Skordas, J. Gaudiello, T. Standaert, H. Jagannathan, D. Corliss, M.-H. Na, A. Knorr, T. Wu, D. Gupta, S. Lian, R. Divakaruni, T. Gow, C. Labelle, S. Lee, V. Paruchuri, H. Bu, and M. Khare, “Stacked nanosheet gate-all-around transistor to enable scaling beyond FinFET,” in *2017 Symposium on VLSI Technology*, 2017, pp. T230–T231, doi:10.23919/VLSIT.2017.7998183.

[7] “Global TCAD Solutions,” *https://www.globaltcad.com*.

[8] A. Rahman, M. S. Lundstrom, and A. W. Ghosh, “Generalized effective-mass approach for n-type metal-oxide-semiconductor field-effect transistors on arbitrarily oriented wafers,” *Journal of Applied Physics*, vol. 97, no. 5, p. 053702, 2005. [Online]. Available: https://doi.org/10.1063/1.1845586

[9] S. Jin, M. V. Fischetti, and T.-w. Tang, “Modeling of electron mobility in gated silicon nanowires at room temperature: Surface roughness scattering, dielectric screening, and band nonparabolicity,” *Journal of Applied Physics*, vol. 102, no. 8, p. 083715, 2007. [Online]. Available: https://doi.org/10.1063/1.2802586

[10] M. D. Ganeriwala, F. G. Ruiz, E. G. Marin, and N. R. Mohapatra, “A compact model for III-V nanowire electrostatics including band non-parabolicity,” *Journal of Computational Electronics*, vol. 18, no. 4, pp. 1229–1235, 2019. [Online]. Available: https://doi.org/10.1007/s10825-019-01389-1

PREPRINT